Available online at www.sciencedirect.com

ScienceDirect

Procedia Structural Integrity 2 (2016) 753–760

Structural Integrity Procedia

www.elsevier.com/locate/procedia

21st European Conference on Fracture, ECF21, 20-24 June 2016, Catania, Italy

Numerical prediction of ductile fracture resistance of welded joint zones

Bashir Younise[a], Marko Rakin[b,*], Nenad Gubeljak[c], Bojan Međo[b], Aleksandar Sedmak[d]

[a] *University of El Mergib, Faculty of Engineering, Khoms, Libya*
[b] *University of Belgrade, Faculty of Technology and Metallurgy, Karnegijeva 4, 11120 Belgrade, Serbia*
[c] *University of Maribor, Faculty of Mechanical Engineering, Smetanova 17, 2000 Maribor, Slovenia*
[d] *University of Belgrade, Faculty of Mechanical Engineering, Kraljice Marije 15, 11120 Belgrade, Serbia*

Abstract

This study deals with the numerical prediction of ductile fracture initiation and development in welded joints of a high strength low alloyed steel. Having in mind the material heterogeneity in the joint zone, a combined experimental-numerical procedure is applied for determination of properties of the weld metal and heat affected zone - HAZ (both coarse-grained and fine-grained portion). Single smooth tensile specimen is tested, and the surface strains are determined during this test using stereometric measurement. Combined with numerical analysis, this enabled determination of stress-strain curves, which are subsequently used in numerical analysis of fracture of pre-cracked specimens. Two different geometries are considered: standard single-edge notched bend (SENB) specimens and surface-cracked tensile specimens. In each of them, the crack is positioned either in weld metal or between the coarse-grained and fine-grained HAZ. Micromechanical model (complete Gurson model, by Z.L. Zhang) is applied in numerical analysis. Higher resistance to ductile fracture initiation and crack growth in HAZ is successfully predicted, as well as constraint effect caused by different crack shapes.

Peer-review under responsibility of the Scientific Committee of ECF21.

Keywords: welded joint; heat affected zone; ductile fracture; numerical analysis; micromechanical model

* Corresponding author. Tel.: +381-11-3303-653; fax: +381-11-3370-387.
E-mail address: marko@tmf.bg.ac.rs

Copyright © 2016 The Authors. Published by Elsevier B.V. This is an open access article under the CC BY-NC-ND license (http://creativecommons.org/licenses/by-nc-nd/4.0/).
Peer review under responsibility of the Scientific Committee of ECF21.
10.1016/j.prostr.2016.06.097

1. Introduction

Ductile fracture is conventionally characterized by fracture mechanics parameters and crack growth resistance curves, obtained from the standard fracture mechanics tests. However, testing of different specimens often reveals considerable differences, due to the constraint effects, as shown by Schwalbe et al. (1997), Kocak (1998), Clausmeyer et al. (1991), Hacket et al. (1993), Kirk and Bakker (1995), Pluvinage et al. (2014). The constraint influences the fracture resistance even in macroscopically homogeneous structures (e.g. dependence on structure/crack geometry and loading type). It is a reason why fracture parameters (such as *J* integral, stress intensity factor, etc.) cannot always be successfully transferred from one geometry to another, for example from laboratory specimens to real machine or structure components.

In welded joints, the problem becomes more complex, having in mind the heterogeneity of the joint zones, in addition to the other constraints. The safety of welded structures in exploitation depends on integrity of their welded joints. Therefore, the fracture resistance of the joint is a very important factor for understanding the fracture and failure of such structures under different exploitation conditions, Kocak (1998), Ravi et al. (2004), Kozak et al. (2009), Chibber et al. (2011), Rakin et al. (2008), Younise et al. (2011), Rakin et al. (2013). In case the crack is located in the middle of weld metal (WM), the joint is often considered as bimaterial - consisting of base metal and weld metal. However, there are situations when it is very important to take into account the fracture behavior of heat affected zone (HAZ), Gubeljak (1999), Wilsius et al. (2006). Its toughness may influence the overall fracture behavior of a welded joint, if the initial defect is positioned in HAZ, or if the crack reaches this zone during the crack growth.

Nomenclature

a_0	initial crack length
Δa	crack length increment
f	current void volume fraction
f^*	modified void volume fraction (damage function)
f_0	initial void volume fraction
f_c	critical void volume fraction
f_u^*	ultimate void volume fraction
f_F	void volume fraction at final failure
f_N	volume fraction of void nucleating particles
f_v	volume fraction of non-metallic inclusions
J	*J*-integral
J_i	*J*-integral at crack initiation
$J_{0.2/BL}$	*J*-integral at 0.2 mm crack growth offset to the blunting line
n	strain hardening exponent
q_1, q_2	fitting parameters of the Gurson-Tvergaard-Needleman yield criterion
r	void space ratio
S_N	standard deviation in the Gaussian distribution of nucleation rate
Greek symbols	
α,β	parameters in CGM
ε_1, ε_2, ε_3	principal strains
ε_N	mean nucleating strain
ϕ	yield function of the Gurson-Tvergaard-Needleman model
Φ	position of the point along the front of the surface crack
λ	mean free path between non-metallic inclusions
σ_1	maximum principal stress
σ_m	mean stress
σ	current flow stress of the matrix material

In this work, resistance to ductile fracture of welded joints of a high strength low alloyed (HSLA) steel is analyzed. The goal was to determine the influence of material heterogeneity, specimen/crack geometry and loading type on the prediction of fracture initiation using the local approach. A combined experimental-numerical procedure (stereometric strain measurement and finite element analysis) is applied to determine the properties of all welded joint subzones on a single tensile plate specimen. The obtained properties are subsequently used in analysis of the fracture of specimens with a pre-crack in the weld metal or heat affected zone. Micromechanical complete Gurson model is applied for prediction of ductile fracture initiation and development.

2. Micromechanical modeling

Different micromechanical models have been developed for predicting the fracture and failure of materials. Among such models dealing with ductile fracture, the one proposed by Gurson (1977) is often used. To be more precise, a version of this model modified by Tvergaard (1981) and Tvergaard and Needleman (1984), has found a rather wide application:

$$\phi\left(\sigma_{\mathrm{eq}},\sigma_{\mathrm{m}},\sigma,f\right)=\left(\frac{\sigma_{\mathrm{eq}}}{\sigma}\right)^2+2q_1f^*\cosh\left(\frac{3q_2\sigma_{\mathrm{m}}}{2\sigma}\right)^2-\left(1+\left(q_1f^*\right)^2\right)=0 \tag{1}$$

Eq. (1) represents the yield function of this model (often called GTN, by the names of its authors); σ_m is the mean stress, σ is the flow stress of the matrix material, f^* is the modified void volume fraction or damage function, and σ_{eq} is von Mises equivalent stress. The constants q_1 and q_2 are fitting parameters introduced by Tvergaard (1981). The damage function f^* is related to the void volume fraction f:

$$f^*=\begin{cases} f & \text{for} \quad f\le f_{\mathrm{c}} \\ f_{\mathrm{c}}+\dfrac{f_{\mathrm{u}}^*-f_{\mathrm{c}}}{f_{\mathrm{F}}-f_{\mathrm{c}}}\left(f-f_{\mathrm{c}}\right) & \text{for} \quad f>f_{\mathrm{c}} \end{cases} \tag{2}$$

where f_c is the critical void volume fraction at the onset of void coalescence, $f_{\mathrm{u}}^*=1/q_1$ is the ultimate void volume fraction, and f_F is the void volume fraction at final failure.

The increase in the void volume fraction, f, during an increment of deformation is partly due to the growth of existing voids and partly due to the nucleation of new voids. One population of voids is considered as primary, and they are assumed to emerge around larger particles (in steels, often non-metallic inclusions), at low loading levels. Therefore, volume fraction of non-metallic inclusions f_v is taken as the initial void volume fraction. On the other hand, secondary voids form around smaller particles in the later stages of loading. Their influence is characterized through volume fraction of void nucleating particles f_N, mean strain for void nucleation ε_N and standard deviation S_N, Chu and Needleman (1980).

A very important feature of the modification of the Gurson model used in this work, the complete Gurson model CGM, is the fact that the critical void volume fraction, f_c, is not a material constant. It is actually calculated during the FE analysis, based on the stress and strain fields. The CGM predicts the onset of void coalescence when the following condition is satisfied, Zhang et al. (2000):

$$\frac{\sigma_1}{\sigma}\ge\left(\alpha\left(\frac{1}{r}-1\right)^2+\frac{\beta}{\sqrt{r}}\right)\left(1-\pi r^2\right) \tag{3}$$

The value of the constant β is 1, while Zhang proposed linear dependence of α on hardening exponent n. σ_1 is the maximum principal stress, and r is the void space ratio:

$$r = \sqrt[3]{\frac{3f}{4\pi} e^{\varepsilon_1+\varepsilon_2+\varepsilon_3}} \Bigg/ \left(\frac{\sqrt{e^{\varepsilon_2+\varepsilon_3}}}{2} \right) \tag{4}$$

where ε_1, ε_2 and ε_3 are the principal strains.

3. Materials

The base metal is HSLA steel NIOMOL 490K; shielded metal arc welding process (SMAW) was applied, and more details can be found in Younise et al. (2012). The shape of the welded joint is K, which was selected in order to make easier positioning of a crack in HAZ.

Precise estimation of true stress - true strain curves for different welded joint regions is difficult due to the heterogeneous properties of the joint zones, especially for heat affected subzones. Therefore, they are obtained by testing a smooth tensile plate, using stereometric measuring system (www.gom.com) and numerical model which includes all joint zones (base metal BM, coarse grain heat-affected zone CGHAZ, fine grain heat-affected zone FGHAZ and weld metal), as shown in Younise et al. (2012). Stress - strain curves obtained by this single-specimen procedure are given in Fig. 1.

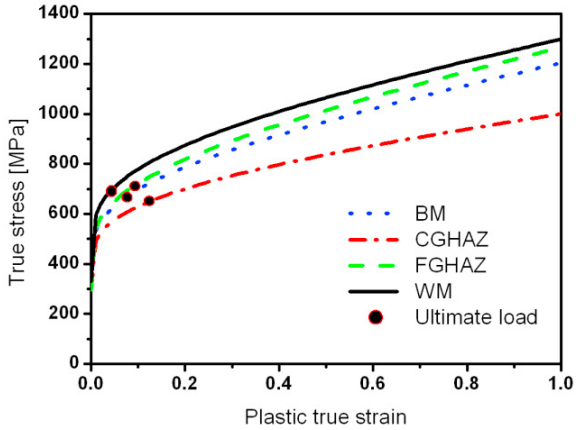

Fig. 1. True stress - plastic strain curves of the welded joint zones

Microstructural parameters are shown in Table 1. Volume fraction (f_v) and mean free path (λ) between the non-metallic inclusions in WM and HAZ are determined by quantitative microstructural analysis, in accordance with ASTM E1245 (2008). The initial porosity f_0 is assumed to be equal to the volume fraction of non-metallic inclusions (f_v), because in the initial stage of ductile fracture of steel, the voids nucleate mostly around these particles. Volume fraction of secondary void nucleating particles f_N (in steel, these are mainly Fe_3C particles) is calculated using the lever rule, Awerbuch (2001).

Table 1.Microstructural parameters of the weld metal and heat affected zone

Parameter	WM	HAZ
f_v	0.0194	0.0086
f_N	0.0107	0.0147
λ [μm]	202	497

Two single edge notch bend (SENB) specimens are used to examine the fracture behavior of joints: with fatigue pre-cracks in WM and HAZ. The initial crack length to specimen width ratio was a_0/W = 0.49 and 0.45 for

specimens with a pre-crack in WM and HAZ, respectively. The cracks were located in the middle of the weld metal or in the middle of HAZ, between CGHAZ and FGHAZ.

Additionally, two surface-cracked tensile specimens are examined, in order to determine the influence of the geometry and loading mode on ductile fracture prediction; positions of the pre-cracks were also in WM or in HAZ. The ratio of crack depth to crack length was 0.25, while the ratio of crack depth to specimen thickness was 0.5 (the crack shape is shown in the next section).

4. Numerical models

Fig. 2 shows the finite element meshes of the specimens with a pre-crack in WM; besides them, the models of specimens with a pre-crack in HAZ are also considered. The loading of both specimens is controlled by prescribed displacements (resulting in either tensile loading or bending due to the contact with the non-deformable bodies).

FEM software package Abaqus (www.simulia.com) is used for numerical analysis, with CGM user subroutine developed by Zhang et al. (2000). In front of the crack tip, finite elements with sizes 0.2 mm (for specimen with a pre-crack in WM) and 0.5 mm (for specimen with a pre-crack in HAZ) are used. These sizes approximate the value of the mean free path between non-metallic inclusions in tested materials (Table 1), and were previously shown as appropriate for fracture prediction in examined joints, Younise et al. (2012).

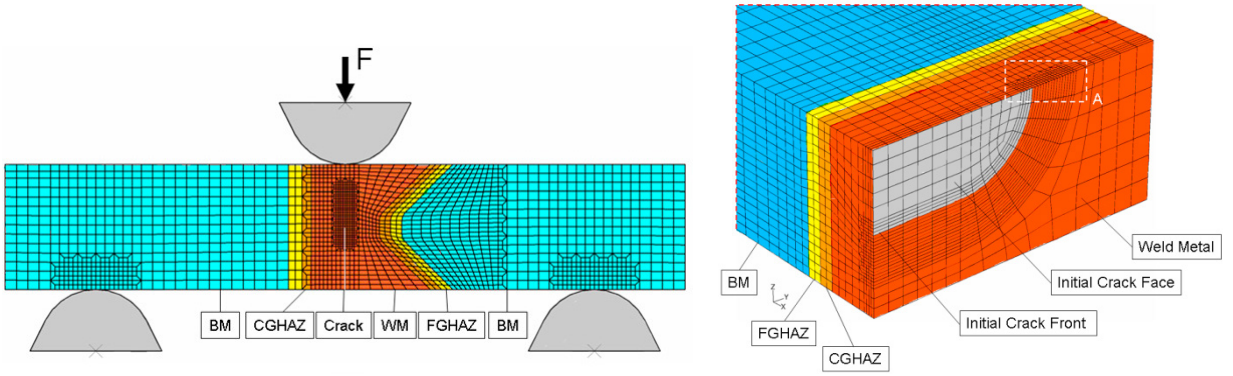

Fig. 2. Finite element models of the specimens with a pre-crack in the weld metal: SENB specimen and surface-cracked tensile panel

CGM model parameters are as follows: constitutive parameters q_1 / q_2, depending on the hardening of the material, are 1.6 / 1.0 (pre-crack in WM) and 1.2 / 1.0 (pre-crack in HAZ), according to Faleskog et al. (1998). Void volume fraction at final fracture (f_F) is determined according to the relation from Zhang et el. (2000). Volume fraction of void nucleating particles (f_N) is determined based on Fe_3C content in materials, and nucleation parameters $\varepsilon_N = 0.3$ and $S_N = 0.1$, Chu and Needleman (1988), Betegon et al (1997) and Dutta et al. (2008), are considered for the analysis.

5. Results and discussion

The influence of the material heterogeneity is predicted using the micromechanical model, as shown in Fig. 3. The fracture resistance of the heat affected zone is much higher in comparison with the weld metal. Unfortunately, one of the properties of the local approach to fracture is dependence of the results on the finite element mesh. The curves in Fig. 3 correspond to the finite element sizes which are obtained as optimal for the weld metal and HAZ, as shown in Younise et al. (2012). The same sizes are subsequently used for assessment of ductile fracture initiation in different geometry - tensile specimen with a surface crack positioned in the weld metal or in the heat affected zone. Therefore, the size of the element is the micromechanical parameter which is transferred to another configuration (different geometry of the structure and crack, as well as different loading mode).

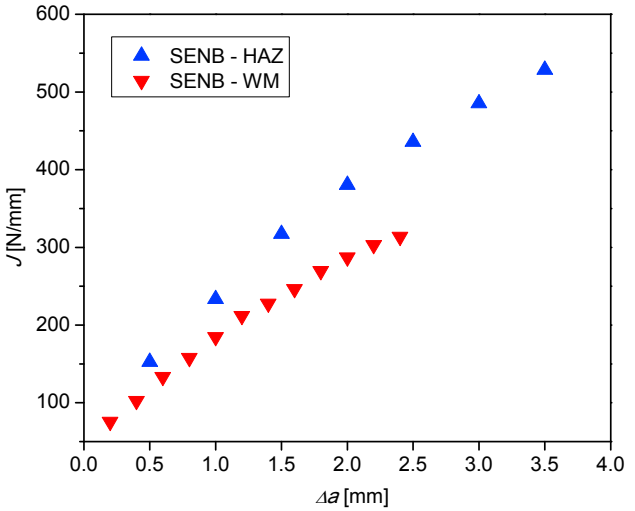

Fig. 3. Crack growth resistance curves for SENB specimens with a pre-crack in WM and HAZ

The J integral value at crack growth initiation (J_i) in numerical analysis is determined by the CGM, at the moment when the critical void volume fraction is reached in the integration point nearest to the crack tip. For tensile panels with a surface crack, there is another issue to be considered - dependence of the fracture conditions on the position of the point along the crack front. In Fig. 4, predicted crack front (using the field of the void volume fraction) is shown, and the position of any point along the crack front is determined by the angle Φ. Now, if we consider the crack growth in different directions, the diagram on the right-hand side of the same figure is obtained. For the analyzed crack geometry (mainly represented by its depth-to-width ratio) and specimen geometry, the most pronounced crack growth is obtained for the value $\Phi = 90°$. Therefore, this point is used for determination of the crack growth initiation, having in mind that the resistance to ductile fracture is the lowest at that position.

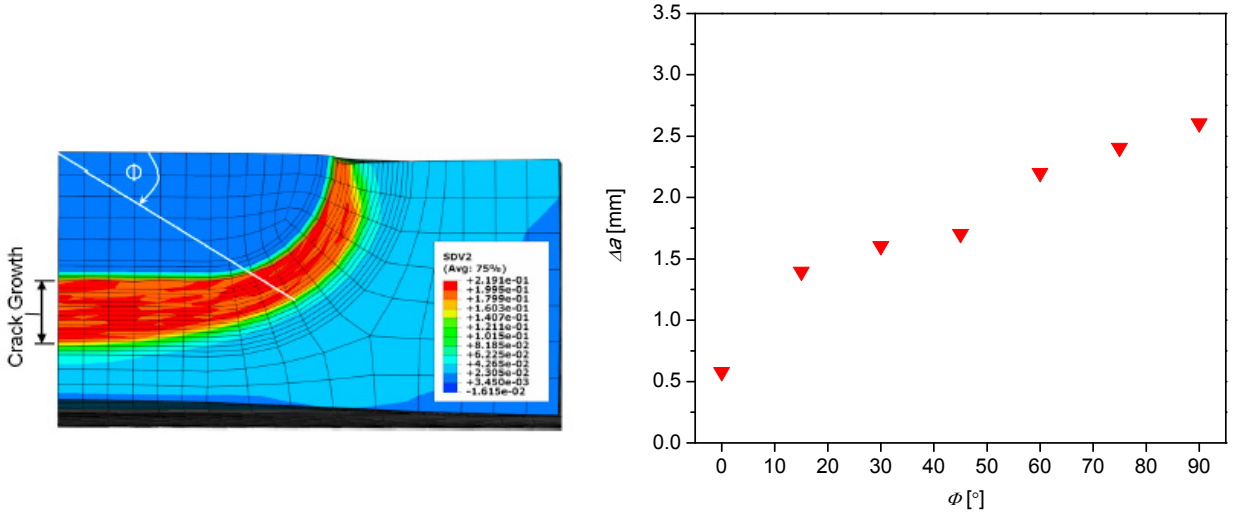

Fig. 4. Crack shape in surface-cracked tensile panel predicted using the CGM and dependence of crack growth on the position (angle Φ) along the crack front

Experimental determination of the critical values of the J integral for SENB specimens is performed according to the standard procedure ASTM E1820 (2008), which means that the value of the J integral corresponding to 0.2 mm crack growth is taken as critical ($J_{0.2/BL}$ - the point position is determined by using the parallel to the blunting line). In the case of tensile panel, the value of J integral at crack growth initiation is determined by the analysis of the stretch zone, i.e. by determining the stretch zone width using the microphotographs of the fractured specimens. This value corresponds to the value J_i, as described in the procedure ESIS P2-92 (1992).

In Fig. 5, all critical values of the J integral at crack initiation, determined experimentally and using the micromechanical model, are shown together. Two geometries of welded specimens are considered, and the cracks are either in weld metal or heat affected zone. From this figure, it can be seen that the micromechanical model can successfully predict the crack growth initiation in the analyzed specimens. The influence of the specimen geometry, crack geometry (passing-through or surface crack) and crack position (in the weld metal or in the heat affected zone) is also obtained. The results shown in this figure are obtained by transferring the micromechanical parameters, initial void volume fraction and finite element size, from one geometry to the other.

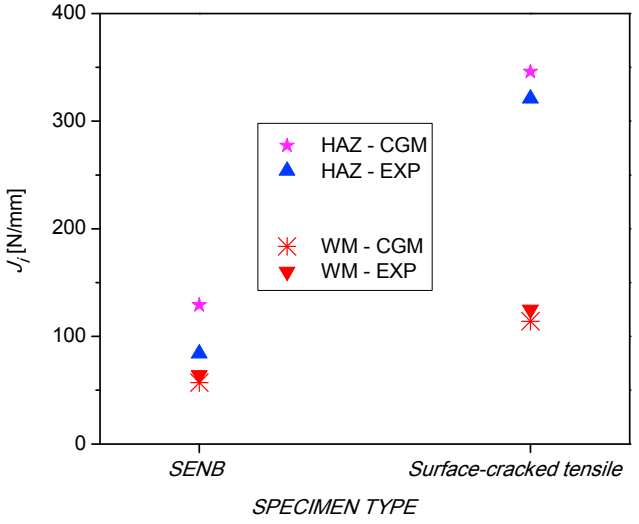

Fig. 5. J integral values at crack initiation for SENB and surface-cracked tensile specimens with a pre-crack in WM and HAZ

6. Conclusions

Geometry and mechanical heterogeneity effect on ductile fracture in welded SENB specimens and tensile surface-cracked specimens with a pre-crack in HAZ and WM has been analyzed using the complete Gurson model (CGM). Fracture resistance is successfully predicted using the CGM and true stress - true strain curves of the welded joint zones, obtained by experimental-numerical procedure (stereometric strain measurement and finite element modeling). It is shown that the resistance to crack initiation and growth is greatly affected by the heterogeneity of the weldment. Also, the micromechanical model successfully predicts the difference in fracture resistance due to material heterogeneity (i.e. position of the crack in the weld metal or heat affected zone), as well as due to the different geometry of the specimen and crack.

Acknowledgements

MR, BM and AS acknowledge the support from the Ministry of Education, Science and Technological Development of the Republic of Serbia under the project ON 174004. The authors would also like to thank Z.L. Zhang for the CGM user subroutine.

References

Awerbuch, J., 2001. Fundamentals of Mechanical Behavior of Materials. Philadelphia: Wiley Custom Publishing.

Betegon, C., Rodriguez, C., Belzunce, F.J., 1997. Analysis and Modelisation of Short Crack Growth by Ductile Fracture Micromechanisms. Fatigue and Fracture of Engineering Materials and Structures 20, 633–644.

Chhibber, R., Biswas, P., Arora, N., Gupta, S.R,. Dutta, B.K., 2011. Micromechanical Modelling of Weldments using GTN Model. International Journal of Fracture 167, 71–82.

Chu, C., Needleman, A., 1980. Void Nucleation Effects in Biaxially Stretched Sheets. ASME Journal of Engineering Materials Technology 102, 249–256.

Clausmeyer, H., Kussmaul, K., Roos, E., 1991. Influence of Stress State on the Failure Behaviour of Cracked Components made of Steel. ASTM Applied Mechanics Review 44, 77–92.

Dutta, B.K., Guin, S., Sahu, M.K., Samal, M.K., 2008. A Phenomenological Form of the q_2 Parameter in the Gurson Model. International Journal of Pressure Vessels and Piping 85, 199–210.

Faleskog, J., Gao, X., Shih, C.F., 1998. Cell Model for Nonlinear Fracture Analysis-I. Micromechanics Calibration. International Journal of Fracture 89, 365–373.

Gubeljak, N., 1999. Fracture Behaviour of Specimens with Surface Notch Tip in the Heat Affected Zone (HAZ) of Strength Mis-matched Welded Joints. International Journal of Fracture 100, 155–167.

Gurson, A.L., 1977. Continuum Theory of Ductile Rupture by Void Nucleation and Growth, Part I . Yield Criteria and Flow Rules for Porous Ductile Media. ASME Journal of Engineering Materials Technology 99, 2–15.

Hackett, E.M., Schwalbe, K.H., Dodds, R.H., editors, 1993. Constraint Effects in Fracture. ASTM STP 1171, ASTM, Philadelphia.

Kirk, M., Bakker, A., editors, 1995. Constraint Effects in Fracture - Theory and Applications: 2nd Vol. ASTM STP 1244, ASTM, Philadelphia.

Koçak M., editor. Weld Mis-match Effect. International Institute of Welding (IIW), IIW Document 1998; X:1419-98.

Kozak, D., Gubeljak, N., Konjatić, P., Sertić, J., 2009. Yield Load Solutions of Heterogeneous Welded Joints. International Journal of Pressure Vessels and Piping 86, 807–812.

Pluvinage, G., Capelle, J., Hadj Méliani, M., 2014. A Review of the Influence of Constraint on Fracture Toughness. Structural Integrity and Life 14, 65–78.

Rakin, M., Gubeljak, N., Dobrojević, M., Sedmak, A., 2008. Modeling of Ductile Fracture Initiation in Strength Mismatched Welded Joint. Engineering Fracture Mechanics 75, 3499–3510.

Rakin, M., Medjo, B., Gubeljak, N. Sedmak, A., 2013. Micromechanical Assessment of Mismatch Effects on Fracture of High-strength Low Alloyed Steel Welded Joints. Engineering Fracture Mechanics 109, 221–235.

Ravi, S., Balasubramanian, V., Babu, S., Nemat Nasser, S., 2004. Assessment of some Factors Influencing the Fatigue Life of Strength Mis-matched HSLA Steel Weldments. Materials & Design 25, 125–135.

Schwalbe, K.H., Ainsworth R.A., Eripret C., Franco C., Gilles P., Koçak M., Pisarski H., Wang Y.Y.,1997. Common Views on the Effects of Yield Strength Mis-Match on Testing and Structural Assessment, in "*Mis-matching of Interfaces and Welds*", GKSS Research Center, Geesthacht, pp. 99–132.

Tvergaard, V., 1981. Influence of Voids on Shear Bands Instabilities Under Plane Strain Conditions. International Journal of Fracture 17, 389–407.

Tvergaard, V., Needleman, A., 1984. Analysis of Cup-cone Fracture in a Round Tensile Bar. Acta Metallurgica 32, 157–169.

Wilsius, J., Imad, A., Nait Abdelaziz, M., Mesmacque, G., Eripret, C., 2006. Void Growth and Damage Models for Predicting Ductile Fracture in Welds. Fatigue and Fracture of Engineering Materials and Structures 23, 105–112.

Younise, B., Rakin, M., Gubeljak, N., Medjo, B., Sedmak, A., 2011. Numerical Simulation of Constraint Effect on Fracture Initiation in Welded Specimens using a Local Damage Model. Structural Integrity and Life 11, 51–56.

Younise, B., Rakin, M., Gubeljak, N., Medjo, B., Burzić, M., Zrilić, M., Sedmak., A., 2012. Micromechanical Analysis of Mechanical Heterogeneity Effect on the Ductile Tearing of Weldments. Materials and Design 37, 193–201.

Zhang, Z.L., Thaulow, C., Odegard, J., 2000. A Complete Gurson Model Approach for Ductile Fracture. Eng Fract Mech 67, 155–168.

ASTM E1245, 2008. Standard Practice for Determining Inclusion Content of Steel and Other Metals by Automatic Image Analysis. American Society for Testing and Materials, Philadelphia.

ASTM E1820-08, 2008. Standard Test Method for Measurement of Fracture Toughness. American Society for Testing and Materials, Philadelphia.

ESIS P2-92, 1992. Procedure for Determining the Fracture Behavior of Materials. European Structural Integrity Society: ESIS Publication.